neuroReport

NeuroReport **8**, 1103–1107 (1997)

Combined EEG and MEG recordings of visual 40 Hz responses to illusory triangles in human

Catherine Tallon-Baudry,[CA] Olivier Bertrand, Christian Wienbruch,[1] Bernhard Ross[1] and Christo Pantev[1]

Brain Signals and Processes Laboratory, INSERM U280, 151, cours Albert Thomas, F-69424 Lyon cedex 03, France; [1]Center of Biomagnetism, Institute of Experimental Audiology, University of Münster, Kardinal-von-Galen-Ring 10, D-48129 Münster, Germany

[CA]Corresponding Author

EEG and MEG were simultaneously recorded to study the visual gamma-band (30–70 Hz) responses. The electrical gamma-band response phase-locked to stimulus onset can be subdivided into a central component at 39 Hz and an occipital component at 36 Hz. A new high-frequency magnetic phase-locked response recorded over the occipital lobe is described. Its topography is complex and probably reflects the activity of multiple sources. Both electrical and magnetic high-frequency responses differ in topography from the low-frequency responses in the same latency range, suggesting that at least partially distinct sources are involved. The existence of a non-phase-locked 40 Hz component around 280 ms is confirmed in EEG data but is not detectable in MEG data.

Key words: 40 Hz; Electroencephalogram; Gamma-band; Human cortex; Magnetocephalography; Synchronization; Temporal code; Vision; Visual

Introduction

An early oscillatory response in the gamma-band (30–70 Hz), phase-locked to stimulus onset (e.g. appearing at a fixed latency), has been described in the auditory modality, in both MEG and EEG recordings.[1,2] More recently, the existence of both phase-locked and non-phase-locked 40 Hz responses was reported from human EEG data in the visual modality.[3–7] The neural structures involved in the generation of these oscillatory activities are not known. In this experiment, we combine EEG and MEG recordings to further characterize these gamma-band visual responses and their relationships to the low-frequency responses appearing in the same latency range. The protocol is the same as in a previous experiment.[6]

Materials and Methods

Four types of stimuli were presented (Fig. 1). The subjects' task was to silently count the occurrences of the curved illusory triangle (target stimulus). Stimulus characteristics were the same as in a previous experiment.[6] Stimuli appeared on screen through a 100×100 fiberoptic matrix. One block of recordings consisted of 50 occurrences of equiprobable non-target stimuli, and 27–34 occurrences of the target stimulus.

Ten subjects (eight females, two males, mean age 27 years) underwent five to six blocks of recordings. Informed consent was obtained from each subject. Recordings were carried out in a magnetically shielded room using a 37 channels neuro-magnetometer (Magnes TM, BTi). The detection coils were arranged in a circular concave array (diameter 144 mm, spherical radius 122 mm) their axes (spacing 22 mm) being normal to this surface. The sensor array was centered approximately midway between electrodes T6 and O2 and positioned as near as possible to the subject's head. Electrical potential were recorded from 17 Ag–AgCl electrodes from the 10-20 system referenced to the nose. Horizontal eye movements were monitored. Continuous EEG and MEG signals were simultaneously recorded at 520.8 Hz (0.03–200 Hz bandwidth). Artifact-free epochs of 350 ms pre- and 650 ms post-stimulus onset were averaged off-line, corresponding to a mean of 153 responses for each type of non-target stimuli and 117 responses for the target stimulus.

To detect and characterize gamma-band oscillatory activities whose latency and frequency ranges are not known *a priori*, we computed a time–frequency (TF) representation of the signal. The method[6–8] is based on a wavelet transform of the signal which provides a time-varying estimate of the energy of the signal around a given frequency f_o. The electrical and magnetic signals are convolved by complex Morlet's wavelets[9] $w(t,f_o)$ having a gaussian shape in both time and frequency domains. The time-varying energy $E(t,f_o)$ of the signal in a frequency band around f_o is the squared norm of the convolution of the complex

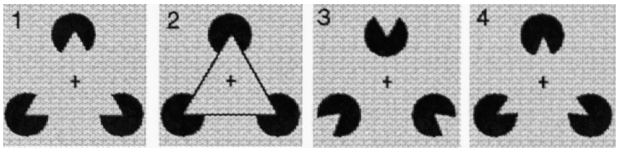

FIG. 1. Stimuli: (1) illusory triangle, (2) real triangle, (3) 'no-triangle stimulus' and (4) curved illusory triangle.

wavelet $w(t,f_o)$ with the signal $s(t)$. Repeating the computation for frequencies ranging from 20 to 100 Hz yields a full TF representation of the signal in this frequency range. The mean TF energy between –200 and –50 ms is considered as a baseline level and subtracted from the pre- and post-stimulus TF energy, independently for each frequency band. The TF energy of each single trial can be averaged, allowing one to analyse both non-phase-locked and phase-locked high-frequency components.

This method can also be applied to the averaged response, providing information only about high-frequency components phase-locked to stimulus onset.

The 'phase-locking factor' enables us to quantify in the time-frequency domain the level of phase-locking of an oscillatory burst, irrespective of its amplitude: this factor ranges from 0 (important latency jitter) to 1 (activity strictly phase-locked to stimulus onset). We averaged, across single trials, the convolution of each complex wavelet with the signal, normalized by its modulus. The modulus of this complex averaged value corresponds to the phase-locking factor in a given TF band. The Rayleigh test of uniformity of angle is used to detect phase ordering.[10]

Because TF energy values are far from having a gaussian distribution, the non-parametric Quade test for related samples and Conover procedures as *post hoc* tests of significance were used.[11] Analysis of variance with Greenhouse-Geiser correction was applied to latency or frequency measurements.

Results

Existence of two distinct electrical oscillatory phase-locked components: For each subject and stimulation type, we computed the TF representation of the phase-locking factor (Fig. 2A). All subjects displayed a significantly phase-locked component ($p < 0.01$) in the 50–150 ms and 25–60 Hz range, at three electrodes at least, and at 10 electrodes on average).

We considered the TF energy of the averaged evoked potential (Fig. 2B) and computed a mean value between 70 and 120 ms and 25 and 50 Hz, at each electrode. Topographical maps of this mean value (Fig. 2C) show an anterior maximum (around Cz) and a bilateral posterior one (T5, T6). No significant variation of this mean value with stimulus type could be found at any electrode (Quade test, $p \leq 0.15$).

The peaking latency and frequency of the phase-locking factor were measured at the electrodes where it reached the significance level of phase-locking ($p < 0.01$). According to the observed topography (Fig. 2C), electrodes were divided into two groups, posterior (OM1, OM2, IZ, T5, T6, O1, O2 and POz), and anterior (P3, PZ, P4, CP1, CP2, C3, Cz, C4 and Fz). The latency of the peak response is about 95 ms and its frequency ranges from 34 to 40 Hz (Table 1). We tested the effects of both topography (posterior/anterior group) and stimulus type on peak latency and peak frequency (two-way ANOVA). The peak latency did not vary with stimulus type ($F = 0.9$, $p = 0.44$), nor with topography ($F = 0.1$, $p = 0.95$). Frequency was not affected by stimulus type ($F = 0.8$, $p = 0.47$), but topography yielded a significant effect ($F = 9.4$, $p = 0.01$). The oscillatory response at 95 ms can thus be subdivided into an anterior component at about 39 Hz and a posterior one at about 36 Hz.

Existence of a complex magnetic phase-locked oscillatory response: All the subjects displayed a significantly phase-locked magnetic component ($p < 0.01$) around 95 ms and 35 Hz (Fig. 3 and Table 1), at 11 sensors at least, and at 26 on average. Stimulus type had no significant effect on either latency ($F = 0.9$, $p = 0.39$) or frequency ($F = 0.8$, $p = 0.46$). Furthermore, the latency of the magnetic response did not differ from the electrical latencies, whether anterior or posterior. The frequency of the magnetic response matched the frequency of the electrical

Table 1. Mean frequency and latency (±s.e.m.) of the maximum of the phase-locking factor, in each experimental condition, grand average across 10 subjects

	EEG, anterior group		EEG, posterior group		MEG	
	Frequency (Hz)	Lat. (ms)	Frequency (Hz)	Lat. (ms)	Frequency (Hz)	Lat. (ms)
Illusory triangle	38.7 ± 2.6	94 ± 7	34.2 ± 2.1	93 ± 6	33.4 ± 1.2	97 ± 2
Real triangle	37.7 ± 1.9	100 ± 6	35.9 ± 2.4	103 ± 5	34.6 ± 0.9	102 ± 2
No triangle	39.9 ± 1.7	91 ± 4	37.9 ± 2.5	92 ± 5	35.3 ± 0.9	96 ± 2
Target stimulus	38.1 ± 1.9	96 ± 5	34.4 ± 1.5	92 ± 6	35.2 ± 1.5	96 ± 5
Mean (four stimulus types)	38.6	95.2	35.6	95.0	34.6	97.7

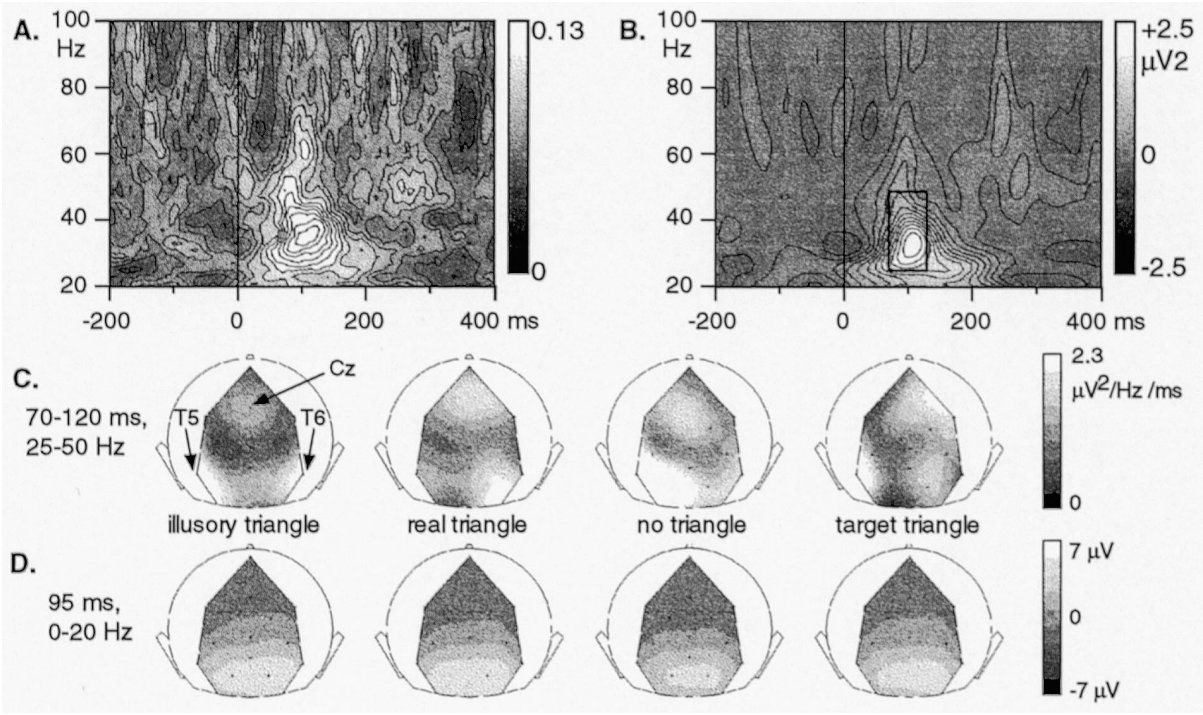

FIG. 2. EEG. (**A**,**B**) Time–frequency representation at electrode Cz in response to the illusory triangle, grand average across subjects. (A) Phase-locking factor. A high value of the phase-locking factor can be observed at about 100 ms and 35 Hz, indicating the existence of a component phase-locked to stimulus onset. (B) Energy of the averaged evoked potential. The frame indicates the 70–120 ms, 25–50 Hz region. (**C**) Topographical maps of the mean 70–120 ms, 25–50 Hz energy of the averaged evoked potential, grand average across subjects. An anterior maximum can be observed at Cz and a bilateral posterior one at T5 and T6. (**D**) Topographical maps of the 0–20 Hz filtered averaged evoked potential at 95 ms, grand average across subjects.

posterior component ($F = 0.5$, $p = 0.51$) but significantly differed from the frequency of the electrical component ($F = 8.42$, $p = 0.02$).

For each subject, the mean 70–120 ms, 25–50 Hz value of the TF energy of the averaged evoked fields was averaged across all sensors. No significant variation with stimulus type could be found (Quade test, $p = 0.36$). For each subject, evoked fields were filtered around the mean frequency found from the phase-locking factor (*f – 5 Hz*, f + 10 Hz). Complex topographies were observed, with a strong inter-subject variability. Fig. 3 shows the example of two different subjects. One subject displays two successive and dipolar topographies reversing in time, while the other one displays two complex, non-dipolar topographies.

Comparison with low-frequency evoked responses (0–20 Hz filtered): The topography of the low-frequency (0–20 Hz) electrical evoked potentials at 95 ms is clearly different from the topography of the high-frequency response (Fig. 2C,D). Moreover, all subjects display very different high- and low-frequency magnetic topographies (Fig. 3). No reliable dipole source localization (one moving or two stationary equivalent current dipoles in a sphere) could be successfully performed on those dipolar or non dipolar-like MEG patterns.

Non phase-locked component of the electrical and magnetic responses: A component around 280 ms and 30–60 Hz can be observed on the electrical TF energy averaged across single trials. It is not phase-locked to stimulus onset (Rayleigh test). In response to the illusory triangle, the mean 220–370 ms, 30–60 Hz TF value averaged across the electrodes located below the sensors (Iz, O2, T6, POz and P4) differs significantly from baseline level estimated from pre-stimulus values (30–60 Hz, –200 to –50 ms) (Wilcoxon test, $p < 0.03$). The same 220–370 ms, 30–60 Hz mean value was measured on the magnetic TF energy averaged across single trials, and averaged across sensors. It did not differ from the pre-stimulus baseline ($p > 0.6$). The magnetic counterpart of the non-phase-locked electrical component was not detectable in these MEG recordings.

Discussion

The electrical 40 Hz phase-locked response at 95 ms can be subdivided into two components, one central (39 Hz) and one occipital (36 Hz). This

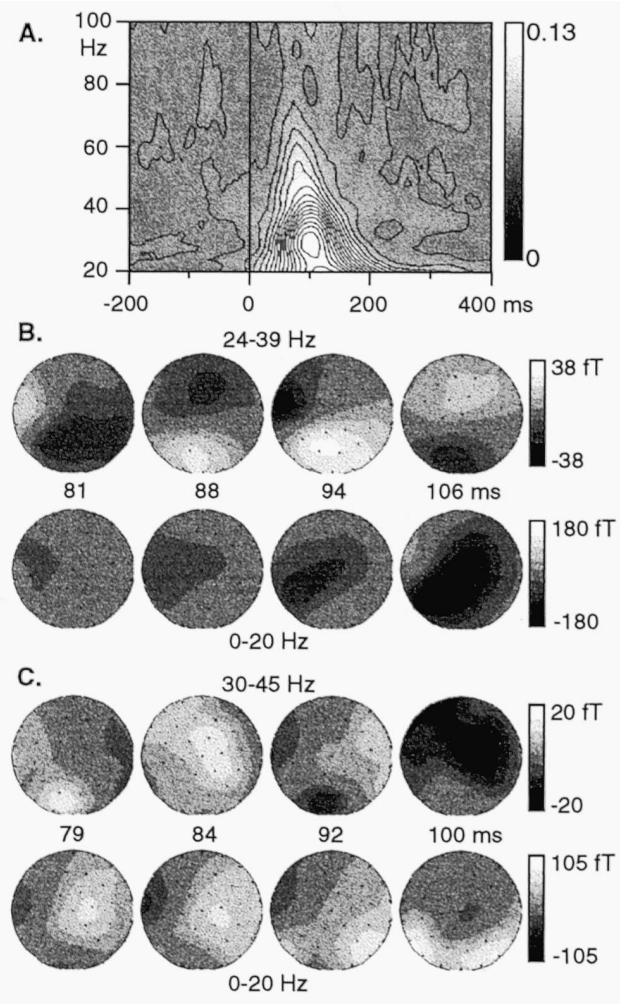

FIG. 3. MEG. (**A**) Time–frequency representation of the phase-locking factor in response to the illusory triangle, grand average across sensors and subjects. (**B**,**C**) Topographical maps of the band-pass filtered (top row) and 0–20 Hz filtered evoked magnetic fields (bottom row) at different latencies. The subject in (B) displays two interleaved dipolar oscillating patterns (81 and 94 ms/88 and 106 ms). The subject in (C) displays two complex, non-dipolar oscillating patterns (79 and 92 ms/84 and 100 ms). The topographies of high- and low-frequency evoked fields are different in both subjects.

finding confirms the results of a previous study[7] and suggests the existence of two distinct groups of oscillating structures in the same latency range. Structures possibly involved could be the lateral geniculate nucleus and V1, where high-frequency activities phase-locked to stimulus onset have been recorded in cats[12] and monkeys.[13]

A magnetic 40 Hz phase-locked response can be recorded over the occipital lobe. Its latency and frequency match those of the occipital electrical response. The complex topography of the gamma-band magnetic response suggests that, even within the occipital lobe, several sources are active. The inter-subject variability observed in MEG data may be partly due to morphological variations of this area.[14] Neither the electrical nor the magnetic phase-locked responses vary with stimulus type.

The sources of the electrical and magnetic high-frequency responses are at least partially distinct from those generating the low-frequency activities in the same latency range, as the topographies of high- and low-frequency responses seem different. This apparent independence of high- and low-frequency evoked responses is in line with the results of Sannita *et al*.[5] The visual gamma-band evoked response differs from the auditory transient 40 Hz response, as the topography of the auditory high- and low-frequency responses are quite similar.[15] In both the auditory and visual modalities, the functional role of the early gamma-band evoked response remains a matter of question, but it does not seem to vary with stimulus type.[6,7,16] This activity could serve as a link between brain regions activated by simultaneous external events.[17,18]

As already observed in previous experiments,[6,7] a non-phase-locked gamma-band component appears around 280 ms on electrical data. However, it was not detectable in our magnetic data. This discrepancy could be due to inappropriate sensor locations and deep and/or radially oriented sources. Furthermore, no polarity inversion of gamma-band oscillations was observed in the cat across cortical layers.[19,20] The EEG/MEG discrepancy could be due to multiple microsinks and microsources, distinct from those leading to the classical current dipole model.

In conclusion, both EEG and MEG techniques enable us to record a phase-locked 40 Hz activity at 95 ms. Electrical data suggest the existence of two groups of oscillating structures, a central one and a posterior one. Magnetic data further suggest that within this posterior group, multiples sources are activated. Moreover, these sources seem to be at least partially different from those generating the low-frequency response in the same latency range. The existence of a non-phase-locked 40 Hz component measured on electrical data is confirmed, but was not detectable in our MEG recordings.

References

1. Galambos R, Makeig S and Talmachoff PJ. *Proc Natl Acad Sci USA* **78**, 2643–2647 (1981).
2. Pantev C, Makeig S, Hoke M *et al. Proc Natl Acad Sci USA* **88**, 8996–9000 (1991).
3. Jokeit H, Goertz R, Küchler E *et al.* Event-related changes in the 40 Hz electroencephalogram in the auditory and visual reaction time times. In: Pantev C, Elvert T and Lütkenhöner B, eds. *Oscillatory Event-related Brain Dynamics*. New-York: Plenum, 1994: 135–146.
4. Tallon C, Bertrand B, Bouchet P *et al. Eur J Neurosci* **7**, 1285–1291 (1995).
5. Sannita WG, Lopez L, Piras C *et al. Electroencephalogr Clin Neurophysiol* **96**, 206–218 (1995).
6. Tallon-Baudry C, Bertrand B, Delpuech C *et al. J Neurosci* **16**, 4240–4249 (1996).
7. Tallon-Baudry C, Bertrand B, Delpuech C et al. *J Neurosci*, in press (1997).
8. Bertrand O, Tallon-Baudry C and Pernier J. Time-frequency analysis of oscillatory gamma-band activity: wavelet approach and phase-locking estimation. In: Wood CC *et al*, eds. *BIOMAG 96: Advances in Biomagnetism Research*. Berlin: Springer-Verlag, in press.

9. Kronland-Martinet R, Morlet J and Grossman A. *Int J Patt Recogn Art Intell* **1**, 273–302 (1987).
10. Jervis BW, Nichols MJ, Johnson TE *et al. IEEE Trans Biomed Eng* **30**, 43–50 (1983).
11. Conover WJ. *Practical Non-parametric Statistics*, 2nd edn. New York: Wiley, 1980: 493.
12. Wörgötter F and Funke K. *Vis Neurosci* **12**, 469–484 (1995).
13. Maunsell JHR and Gibson JR. *J Neurophysiol* **68**, 1332–1344 (1992).
14. Thompson PM, Schwartz C, Lin RT *et al. J Neurosci* **16**, 4261–4274 (1996).
15. Bertrand B and Pantev C. Stimulus frequency dependence of the transient oscillatory auditory evoked responses (40 Hz) studied by electrical and magnetic recordings in human. In: Pantev C, Elbert T and Lütkenhöner B, eds. *Oscillatory Event-related Brain Dynamics*. New York: Plenum, 1994: 135–146.
16. Tiitinen H, Sinkkonen J and May P. *NeuroReport* **6**, 190–192 (1994).
17. Joliot M, Ribary U and Llinas R. *Proc Natl Acad Sci USA* **91**, 11748–11751 (1994).
18. Leonards U, Singer W and Fahle M. *Vis Res* **36**, 2689–2697 (1996).
19. Steriade M, Amzica F and Contreras D. *J Neurosci* **16**, 392–417 (1996).
20. Steriade M and Amzica F. *Proc Natl Acad Sci USA* **93**, 2533–2538 (1996).

ACKNOWLEDGEMENTS: This work was supported by grants from the Human Frontier and Science Program (RG-20/95B) and from the french ministry of research (ACC-SV 12 functional brain imaging).

Received 19 November 1996; accepted 30 January 1997

General Summary
Phase-locked and non-phase-locked gamma-band (30–70 Hz) EEG responses have been recently described in the visual modality. In this study, we combine EEG and MEG recordings to further characterize these oscillatory responses. The electrical phase-locked response at 95 ms can be subdivided into two components at different frequencies, an anterior one (39 Hz) and a posterior one (36 Hz). A new magnetic oscillatory phase-locked response recorded from the occipital lobe is described. Its frequency matches the frequency of the posterior electrical response. Its topography is complex, suggesting that even within the occipital lobe, multiple sources are involved. The topography of both the electrical and magnetic high-frequency responses differs from the topography of the low-frequency responses : high- and low-frequency activities around 100 ms are probably generated by at least partially distinct sources. A non phase-locked gamma-band response around 280 ms can be observed in EEG data, but not in MEG data.